Title: Sustained Release of Cx43 Antisense Oligodeoxynucleotides from Coated Collagen Scaffolds Promotes Wound Healing

Authors: Daniel J. Gilmartin, Allyson Soon, Christopher Thrasivoulou, Anthony RJ Phillips, Suwan N. Jayasinghe and David L. Becker*

Address:

DL Gilmartin, PhD, C Thrasivoulou, PhD, SN. Jayasinghe, PhD.

Department of Cell and Developmental Biology, University College London, London, WC1E 6BT, UK

ARJ Phillips, MD, PhD.

School of Biological Sciences, Department of Surgery, University of Auckland, New Zealand.

A. Soon, PhD, DL. Becker PhD.

Lee Kong Chian School of Medicine, Nanyang Technological University, 11, Mandalay Road, Singapore, 308232.

And DL. Becker PhD.

Institute of Medical Biology, A*STAR, 8A- Biomedical grove, Biopolis, Singapore 138648

e-mail: David.becker@ntu.edu.sg

Key words:

Oligonucleotide Delivery, Tissue Repair, Scaffold,

Abstract:

Antisense oligodeoxynucleotides targeting the mRNA of the gap junction protein Cx43 have been shown to promote tissue repair in a variety of different wounds. Delivery of the antisense drug has most often been in a thermo-reversible hydrogel, Pluronic F-127, which is very effective in the short term but does not allow for sustained delivery over several days. For chronic wounds that take a long time to heal repeated dosing with the drug might be desirable but is not always compatible with conventional treatments such as the weekly changing of compression bandages on venous leg ulcers. Here we investigated the coating of collagen scaffolds with antisense and found a way to provide protection of the oligodeoxynucleotide drug in conjunction with sustained release over a 7 day period. This approach significantly reduced the normal foreign body reaction to the scaffold, which induces an increase of Cx43 protein and an inhibition of healing. As a result of the antisense integration into the scaffold, inflammation was reduced with the rate of wound healing and contracture significantly improved. This coated scaffold approach may be very useful for treating venous leg ulcers and also providing a sustained release of any other types of oligonucleotide drugs that are being developed.

Introduction

Chronic wounds such as venous leg ulcers and diabetic foot ulcers are a growing problem world wide as our population grows older and more obese and the incidence of diabetes continues to rise to epidemic levels (Farag and Gaballa, 2011; Mustoe, 2004; Nunan et al., 2014). These hard to heal wounds are often deep with loss of all skin tissue layers, and have profound effects on the life style of patients who all too often end up with lower limb amputations. The cost to healthcare services is a severe burden and it is estimated to cost over $25B each year in the USA alone (Sen et al., 2009). Similarly deep burns can result in a significant loss of tissues and wounds that can be very slow to heal. Tissue grafting is a solution but in severe burns there may not be sufficient intact skin for an autograft and even then, only 50% of grafts on average will take (Atiyeh and Costagliola, 2007). To overcome this problem artificial scaffolds have been designed to encourage complex tissue regeneration and improve wound healing (Zhong et al., 2010).

The complexity of scaffolds varies considerably from a simple spun collagen matrix to a living artificial skin seeded with living human keratinocytes, such as Apligraf® and Orcel® (Bioscience). The complex living scaffolds however, have several drawbacks in terms of shelf life and manufacturing cost. Simpler scaffolds on the other hand may act as little more than a dressing. Indeed we have previously shown that several forms of simple spun alginate or collagen scaffold, or microspheres, can induce a foreign body reaction at the wound edge, which can further retard the healing process (Gilmartin et al., 2013). As part of the foreign body inflammatory reaction there is an elevation of the protein levels of the gap junction connexin 43 (Cx43) in the wound edge keratinocytes and fibroblasts, which is known to inhibit the migration of these cells. Soaking the scaffolds in a thermo-reversible Pluronic gel containing Cx43 antisense oligodeoxynucleotides (Cx43asODN's)

resulted in a transient bioactivation of the scaffold and alleviated some of the foreign body reaction and encouraged outgrowth of the wound edge keratinocytes. However, the gel associated with the scaffold was short lived and soon the inflammatory response returned and the scaffold was attacked by leukocytes. A scaffold that could be coated to elute a drug or drugs over several days would be very desirable.

A number of vascular stents have been developed to incorporate therapeutic drugs that elute from the devices over a pre-determined period of time (Krucoff et al., 2008; Mehilli et al., 2006; Windecker et al., 2008). These are termed ‘drug-eluting stents’, and typically comprise a polymer coating containing the drug that in turn surrounds a traditional metal stent frame. These stent devices aim to provide both structural support to the blood vessel as well as a bioactive component to prevent restenosis. Designing an antisense eluting scaffold coating for an open wound, has not, as far as we are aware, been attempted before and required investigation into the various properties of different polymers. The choice of polymer used to generate stent coatings varies, and is selected based on biocompatibility as well as the rate at which drugs elute from them. PLGA is a copolymer of poly lactic acid (PLA) and poly glycolic acid (PGA), and is one of the most commonly used synthetic polymers in the field of biomaterials. One of the main reasons for its popularity is its reported level of biocompatibility, illustrated by its FDA approval status (Makadia and Siegel, 2011). The approval status of PLGA is due to the breakdown of the polymer into lactic and glycolic acid, both of which are naturally metabolised to carbon dioxide and water through the Krebs cycle. As an additional advantage, the lactide to glycolide ratio of PLGA can also be adjusted to influence the rate of drug elution (Shive and Anderson, 1997). A ratio of 50:50 lactide to glycolide has been reported to elute incorporated drugs at a higher rate than when using a 75:25 ratio, for instance. The use of

Polycaprolactone (PCL) in drug coatings is also well documented, and is reported to elute incorporated drugs at a slower rate than PLGA.

While vascular stent coatings have been designed to release large drug molecules such as paclitaxel, (Krucoff et al., 2008) the release of asODN from coatings is less common as a method to target restenosis (Khan et al., 2004). Examples of asODN eluting stent coatings previously developed include those targeting the DNA binding protein c-myb, platelet derived growth factor, and non-muscle myosin heavy chain, with some leading to positive results both *in vitro* and *in vivo* (Kipshidze et al., 2005). Results from other studies indicate that asODN may elute faster than traditional anti-restenosis drugs, but 32-mer sequences were also found to elute at a slower rate from polymer microspheres than smaller 7-mer or 15-mer sequences (Khan et al., 2004). Since the Cx43asODN sequence in this current study is a 30-mer, it is likely to have a slower release profile.

Here we examine the release properties of different formulations of coatings on a collagen scaffold with the aim of generating a coating that would release our Cx43asODN at a steady rate over a period of 7 days. We hypothesized that sustained release of Cx43asODN would (1) promote sustained re-epithelialization, by downregulating Cx43 at the wound edge (Mori et al., 2006; Qiu et al., 2003; Wang et al., 2007) throughout the 7-day window, and (2) additionally reduce the inflammation and foreign body response, as manifested by neutrophil cell infiltration and abnormal epithelial wound edge thickening near the scaffold.

Results:

Polymer coating and antisense elution

Scaffolds were initially coated using either a 10% or 15% (wt./v.) solution of PLGA and asODN 100 µM (Fig 1A). Scaffolds were then submerged in 40 µl nuclease free water

and assayed for DNA elution at daily intervals for 4 days (Fig 1B). By the D2 time point over 95% (approximately 10 µg) of DNA had eluted for both 10% and 15% PLGA coated scaffolds. Wounds of 6 mm in diameter, depth 0.7 mm have a volume of 19.8 mm^3. DNA elution from both the 10% and 15% PLGA coatings was calculated to produce an effective asODN concentration of 54.4 µM in the wound bed.

In order to both prolong the duration and quantity of asODN release, the asODN loading concentration was increased to 300 µM. Three new combinations were produced for evaluation: i) scaffolds coated using just 15% PLGA and the Cx43asODN, ii) scaffolds coated in 10% PCL and Cx43asODN or iii) a combined approach of a layer of PCL + Cx43asODN, followed by a layer of PLGA + Cx43asODN (Fig1C). Elution profiles were then studied over a 7 day period (Fig1D). For single coating of PCL, elution of asODN occurred more gradually than from the single PLGA coating. The PCL-only group, eluted 19 µg of DNA in 7 days, with half released after 1 day, as compared to 15 h for half of the DNA from the single PLGA coating. Scaffolds that received the combination of PCL and PLGA coatings eluted approximately 48 µg of asODN over the course of 7 days of which half eluted within 24 h. Elution of 48 µg released at once into a typical 19.8 mm^3 wound volume, was calculated to produce an effective concentration of 260.4 µM .

For PCL only four coat scaffolds, half of the asODN eluted by 2.5 days, relative to just 1 day for the single coating. The most noticeable change in performance between one and four layering coatings, however, was found using the PCL and PLGA double-coated scaffolds. This coating resulted in an average 7-day total release of 265 µg, which was considerably greater than the coatings of only PCL or PLGA. When asODN elution from combination-coated scaffolds was assessed on a day-by-day basis as opposed to cumulative release, there were two clear peaks of asODN elution in the first 24 hours and then between D3 and D4 (Fig 1E).

The results from the elution assays identified the 4-layered combined PCL and PLGA coating as suitable for testing of function *in vivo*.

In order to evaluate the integrity of asODN incorporated into the polymer coatings, Förster resonance energy transfer (FRET) imaging was used. Collagen scaffolds were generated that were loaded with asODNs labelled with the dye Cy5 at the 3’ terminus and the Cy3 dye at the 5’ terminus which were capable of FRET when intact (Fig 2A). Immediately after

coating scaffolds, FRET efficiency was calculated to be 25%, (Fig 2 B & D) which previous studies have accepted as genuine (Lai et al., 2014). In order to assess whether asODN contained within the coatings was afforded a degree of protection against nuclease activity present in wounds, a series of FRET asODN coated scaffolds were submerged in foetal bovine serum (FBS) at 37°C for 7 days. Scaffolds were harvested every 24 h and FRET efficiencies were determined for 6 individual asODN clusters per time point (Fig 2B). The average FRET efficiencies calculated between D1 and D7 ranged from 17.5 % - 26.7%, in all cases remaining above 15% (Fig 2B).

In order to confirm that FRET was not occurring due to inadequate nuclease activity of the FBS used, FRET labelled Cx43 asODN was mixed with FBS for 6 h at 37°C. A lambda scan was then performed on the FRET-FBS solution on a Leica confocal microscope, using a 533 nm laser to stimulate CY3. A second lambda scan was performed on a control solution of FRET labelled asODN that had been mixed with water and the two scan outputs were compared. The resultant scans showed a second peak of emission between 650-680 nm in the control asODN solution, yet this peak was absent in the solution treated with FBS indicating that the asODN had been broken down (Fig 2C).

Using coated scaffolds to deliver Cx43 asODN to wounds

In order to compare the *in vivo* effects of Cx43asODN in the polymer coated scaffolds accurately, a series of control scaffolds were devised to allow comparisons (Fig 3A). These consisted of an uncoated scaffold, as well as two additional polymer coated scaffolds, one without asODN (‘coated only scaffold’) and the other with a sense sequence to Cx43sODN (‘Cx43sODN scaffold’). Full-thickness 6 mm wounds were made to the backs of rats and individual scaffolds were applied (n=8 per treatment and time point).

Wounds at D1, 3 and 5 that received uncoated scaffolds were typically larger than any of the other treatments (Fig 3B). At D1, all scaffolds appeared to prevent wound contraction to some degree. However, by D3 wounds treated with Cx43asODN scaffolds appeared markedly reduced in size compared to the control scaffolds and were similar to untreated wounds. Wounds treated with uncoated scaffolds at D3 were similar in size to the initial wound. Coated scaffolds typically showed signs of breakdown to varying degrees at both D3 and D5, but wound edges did not appear to integrate with coated scaffolds. By D5,

wounds treated with the Cx43asODN scaffolds had reduced in size considerably, often to a greater degree than untreated wounds.

Re-epithelialisation and connexin expression analysis

Day 1

At D1, untreated wounds had re-epithelialised on average a distance of 274 µm (Fig 4B). This was greater than control scaffold-treated wounds (uncoated, coating only, and coated + Cx43sODN), which had re-epithelialised on average a distance of 202 µm, although the difference was not significant. Wounds treated with scaffolds coated in Cx43asODN, however, had re-epithelialised significantly further, an average distance of 407 µm, this was 67% greater than untreated wounds ($P < 0.01$) and 101% greater than the combined averages of the control scaffold-treated wounds.

Sections of wound edge tissues were immunostained for Cx43 and Cx26 and protein levels of connexins quantified and normalised to a region of distal epidermis. At D1 there was a strong upregulation of Cx26 in wound edge keratinocytes across all conditions, including wounds left untreated, with no significant differences observed between groups (Fig 4A**).** In Cx43asODN coated scaffolds, wound edge epidermis Cx26 was 38% lower than untreated wounds and 57% less than the average of all three control scaffold-treated wounds (Fig 4D). Staining for Cx43 revealed a different outcome. At D1, application of each of the control scaffolds resulted in an increase in Cx43 expression in the wound edge epidermis, with an average increase of 141% over distal levels (Fig 4C). Untreated wound edges displayed a typical downregulation of Cx43 expression by 35%, while Cx43asODN coated scaffold wound edge expression was reduced by 85%. All three control scaffold treatments showed significantly more Cx43 than the untreated control wounds ($P < 0.05$).

Day 3

At D3, untreated wounds had re-epithelialised an average of 522 µm, whilst the average was 389 µm for the combined distances of control scaffold-treated wounds (Fig 5A & B). Wounds treated with the Cx43asODN scaffolds had again re-epithelialised an average distance of 859 µm, 65% greater than untreated wounds ($P < 0.001$) and 121% greater than the averaged distance for all control treated wounds.

At D3, wound edge keratinocyte Cx26 expression across all treatments was upregulated from the minimal levels observed in uninjured distal epidermis (Fig 5A & D). Uncoated scaffolds produced the highest increase in wound edge Cx26 expression, at 6370%. Cx26 levels were similar between the coated control scaffolds and untreated wounds. Wounds treated with Cx43asODN scaffolds resulted in lower Cx26 expression of only 375% increase at the wound edge at D3 but due to the large variation seen in untreated controls this did not reach significance. Cx43 expression at D3 showed a 65% downregulation in wound edges treated with Cx43asODN scaffolds, comparable to untreated wounds Fig 5A & C). There was a significant elevation in Cx43 protein levels in all the control scaffold groups compared to the untreated control; uncoated scaffolds (335% increase, $P < 0.001$) and Cx43sODN coated scaffolds (283% increase, $P < 0.001$), un-coated scaffolds ($P < 0.05$).

Day 5

Similar measurements were also recorded at D5. At this time point a small proportion of wounds were approaching the final stages of re-epithelialisation, where the epithelial barrier is restored. Untreated wounds had re-epithelialised an average distance of 882 μm, which was only 12% higher than the averaged distance of 779 μm for all control scaffold-treated wounds (Fig 6A). Cx43asODN coated scaffold wounds had re-epithelialised on average 1345 μm, which was a 65% increase over untreated wounds ($P < 0.01$). The increase was again more pronounced over all the control scaffold treatments – Cx43asODN scaffold-treated wound re-epithelialisation was 70% higher than the average of the three control scaffold treatments. Scaffolds coated with polymers containing Cx43asODN resulted in significantly increased levels of wound re-epithelialisation across all the studied time points.

While wound edge Cx26 levels were greatly reduced from those at D3 across all treatments, only the application of Cx43asODN coated scaffolds resulted in a decrease in wound edge Cx26 expression from distal levels (Fig 6A & D). All three control scaffolds resulted in a similar increase in wound edge Cx26 expression, with an average rise of 147%. Both coated and uncoated control scaffolds resulted in higher Cx26 levels than the Cx43asODN scaffold-treated wounds.

Wounds treated with Cx43asODN at D5 maintained a downregulation of Cx43 in wound edge keratinocytes, with a 91% decrease in expression from distal levels (Fig 6A & C). This was lower than untreated wound edge keratinocytes, which displayed a 57%

downregulation of Cx43 at the same time point. Both uncoated and coated scaffolds resulted in significantly higher levels of Cx43 expression than untreated wounds ($P < 0.05$ and $P < 0.01$), although significance was not achieved against the sODN coated scaffold owing to high group variability. While scaffolds appeared to have an effect on keratinocyte Cx43 levels over several days, no clear differences were observed in fibroblasts within the developing granulation tissue at this time point.

Assessment of the foreign body reaction and inflammation

The assessment of thickening in the skin wound of the leading edge (first 150 µm) of the nascent epidermis was also measured as a component of the foreign body reaction and inflammation assessment. At D1, the average thickness of wounds treated with uncoated scaffolds was 107.5 µm (±9.1 µm), which was considerably thicker than untreated at 50 µm (Fig 7A). Coating the scaffolds alone or with Cx43sODN reduced the thickness slightly to 79.5 µm (± 17 µm) and 61.7 µm (± 11 µm), respectively. However, Cx43asODN coated scaffolds produced the thinnest epidermis at 27.8 µm (±6.2 µm). This trend continued at D3 when the untreated wounds averaged a thickness of 70.3 µm (± 11.3 µm), which was similar to coated scaffolds or Cx43sODN scaffolds but thinner than the uncoated scaffolds at 135.3 µm (± 11.3 µm). The Cx43asODN coated scaffold was still the thinnest at 39.7 µm (± 3.7 µm). D5 was similar, with Cx43asODN scaffolds producing the thinnest epidermis at 29.3 µm (±3.8 µm), with untreated wounds at 49.8 µm (± 4.7 µm), similar to coated scaffolds or Cx43sODN scaffolds. Again uncoated scaffolds were the thickest at 141.7 µm (±15.2 µm).

Polymorphonuclear leukocytes (PMNs) were identified and counted in the intact dermis distal to the wound edge in order to investigate the inflammatory response to the scaffolds (Fig 7B). At D1 untreated wounds had an average of 24.8 (± 7.4) PMN cells per field of view which was reduced a little for Cx43asODN coated scaffolds at 15.6 (± 1.3) cells (Fig 7C). However, uncoated scaffolds generated the highest inflammatory response with 66.4 (± 9.9) PMN cells, and coated and sODN coated also causing inflammation with 39 (± 2.9) and 53.8 (± 5.9) PMN cells respectively. At D3, there was slightly elevated numbers of PMNs compared to D1 for all treatments. Again, counts in untreated wounds Cx43asODN coated scaffolds were similar at 20.2 (± 2.7) and 18.8 (± 4.1) PMN cells respectively. Uncoated scaffolds had the highest number of PMNs at 71.2 (± 12.5) with coated and sODN coated similar at 48.6 (± 4.3) and 61 (± 5.3) PMNs respectively. By D5, PMN levels

in distal dermis had decreased considerably across all treatments, including uncoated scaffolds. However, this was still significantly higher than untreated wounds. Cx43asODN coated scaffolds still produced the lowest PMN counts of 9.4 (± 2.5) slightly lower than untreated wounds at 15.2 (± 4.3). Uncoated scaffolds still had the highest inflammation with 35 (± 7.3) PMN cells with coated and sODN coated producing 23.8 (± 2.1) and 31.2 (± 5.4) PMN cells respectively, showing that inflammation was finally resolving.

Granulation tissue formation following scaffold application

Wounds harvested at D10 and D15 were sectioned, H&E stained and the granulation tissue area measured using ImageJ (Fig 8 A). At D10 there were significant differences in the granulation tissue between the scaffold treatments (Fig 8 A & B). Treatment of wounds with Cx43asODN coated scaffolds resulted in an average area of 2.30 μm^2, which was significantly less than untreated wounds (3.61 μm^2, $P < 0.01$). The granulation tissue of coated and sODN coated scaffolds were similar to untreated wounds at 3.47 μm^2 and 3.41 μm^2 respectively. However, uncoated scaffold treated wounds had a significantly larger granulation tissue area at 4.47 μm^2 than untreated wounds ($P < 0.05$).

The positive effect of the bioactive scaffold on wound healing continued to be seen at D15 when wounds had a granulation tissue area of 1.391 μm^2 (Fig 8 C), which was significantly lower than the 2.29 μm^2 of untreated wounds ($P < 0.05$). The granulation tissue area of all the other treatments were very similar with uncoated scaffold (2.70 μm^2), coated scaffold (2.33 μm^2) and sODN coated scaffold (2.39 μm^2).

Discussion:

We have successfully fabricated a scaffold that continuously releases Cx43 asODN over 7 days. This sustained release of Cx43 asODN has (1) continued to promote re-epithelialization by downregulating Cx43 by on average 85% at the epidermal wound edge throughout the 7-day window, and (2) additionally it reduced the foreign body and inflammatory response (evaluated by PMN cell infiltration and epithelial thickening) (3) allowed contraction and closure of the wound at a normal rate or faster than the untreated scaffold.

The initial method of coating scaffolds with a single layer of PLGA containing 100 μM Cx43asODN was insufficient since it released over 95% of the total asODN within the first 48 h. This was improved upon by collagen scaffolds coated with 4 layers of PLGA containing Cx43asODN, where the amount of asODN eluted within the first 3 days approximately tripled. Despite this, over 95% of asODN still eluted within the first 72 h, indicating that the PLGA used in the study may not be sufficient to achieve sustained release of Cx43 asODN.

Scaffolds coated in four layers of PCL, produced a more sustained release profile in which asODN elution only began to plateau at around 6-7 days. This outcome is in agreement with the results of a study performed by (Acharya et al., 2012) where they found that the use of PCL resulted in a more sustained release profile than PLGA or polyethylene glycol. While coating scaffolds with 4 layers of PCL resulted in a sustained release of asODN, coating them with an additional 4 layers of PLGA ('double coat') achieved the greatest overall release of Cx43asODN across the 7-day assessment. Additionally, the elution profile for double coated scaffolds appeared to adopt the characteristics of both the individual PLGA and PCL coatings. There was a large burst release of asODN in the first 24 h characteristic of PLGA as well as the more sustained release profile of PCL throughout the 7-day assessment. This includes a small peak of elution around 3-4 days, which was also present in the PCL-only coated scaffold, and could be explained by hydrolysis of the scaffold coating(Tarvainen et al., 2002). Second peaks of elution have also been found using other multi-layered approaches, such as two-layered scaffold fibres containing an inner layer of PLGA mixed with gentamicin, lidocaine and vancomycin, and a blank outer layer (Chen et al., 2012). The occurrence of a second peak appears to be linked to the use of multiple layers, and may be the result of sufficient hydrolysis of outer layers to expose the inner layers. The initial burst release of asODN observed could be useful in a wound setting as Cx43 must be downregulated to attenuate inflammation and for the re-epithelialisation process to initiate (Mori et al., 2006).

The finding that multiple coating layers improved the overall duration of asODN elution is also in agreement with the results of a clinical trial study that used multi-layered stent coatings with other drugs. In this study, stents were coated with an inside polymer layer

containing Sirolimus as well as an outer layer containing no drug (Schofer et al., 2003). The group found that the use of an outer coating provided a barrier, which slowed the elution of drug from the inner layer so that 80% of the drug eluted over a 30-day period following implantation.

It is important to note, however, that the *in vitro* assessment of elution dynamics serves only as a guideline to estimate in vivo asODN elution. Previously we have found that cross-linked collagen scaffolds are enzymatically degraded in wounds, with significant degradation having typically occurred by D5 (Gilmartin et al., 2013). The harsh wound environment may result in a greater rate of elution than that observed when performing *in vitro* assays. However, coating layers containing drugs have been reported to incompletely release all their drug contents, with one study finding that as much as 25% of the incorporated drug, tacrolimus, remaining in a single layered coating (Wieneke et al., 2003).

While spectrophotometry-based elution profiling showed that a considerable quantity of asODN eluted from PCL-PLGA double-coated scaffolds over 7 days, it did not reveal whether the homogenisation and solvent processing steps performed in the coating process damaged the structure of the incorporated DNA. The FRET acceptor photobleaching was performed on sectioned scaffolds coated using a Cy3 and Cy5 dual labelled Cx43asODN sequence. This technique has been successfully used to study asODN integrity and is favoured for both its accuracy and simplicity (Cronin et al., 2006; Rupenthal, 2012). Immediately after coating (0 h) there was a FRET efficiency of 25.9%. A minimum efficiency of 15-20% has been previously used as an indicator that the FRET occurring was genuine, while lower percentages may reflect background variation (Lai et al., 2014). A FRET efficiency of 25.9% obtained for the double-coated scaffold can be interpreted to mean that the coating contained intact asODN, confirming that the coating process did not render the incorporated asODN non-functional. In order to test whether the multiple coatings afforded a level of protection against DNA degradation, FRET-labelled scaffolds were submerged in fetal bovine serum for up to 7 days and assessed each day to expose them to the DNAase activity of the serum. This revealed similarly high FRET efficiencies within the inner coating layers of scaffolds, even after several days in serum containing nuclease enzymes. The ability of serum enzymes to degrade DNA was also confirmed through a series of lambda scans which showed that serum treated asODN

did not produce the same FRET peak, which suggests that the FBS used was effective in degrading free asODN.

The development of a combined PLGA and PCL coating resulted in an average asODN elution of 265 µg within 7 days in a sustained manner. In order to test whether scaffolds were similarly effective *in vivo* they were applied to 6 mm full-thickness wounds, this time made to the dorsum of rats. Macroscopically, scaffolds coated in the synthetic polymers appeared to integrate poorly with the wound edge, a feature possibly due to the coating layers producing a more rigid scaffold. Scaffolds were loosely associated with wounds, and during processing to permit histological analysis it was not uncommon for scaffolds to separate from wounds. However, at D3 and D5 the Cx43asODN coated scaffold-treated wounds appeared to reduce in size and shrink in the wound compared to the uncoated scaffold-treated wounds. This could be due to the fact that the coating method used did not have cross-linking of scaffolds, thereby permitting the collagenous fibres in the scaffold to break down more rapidly in conjunction with wound contraction. Scaffolds that had been coated without Cx43asODN or coated with sense ODN at D3 and D5 appeared to prevent wound closure to a small degree, relative to untreated wounds. The smallest wounds were those treated with Cx43asODN, which is consistent with previous studies, which have shown how it promotes wound healing and cell migration (Mori et al., 2006; Qiu et al., 2003). Cx43 knockdown has been shown to be accompanied by enhanced activity of the Rho GTPases RhoA, which regulates fibroblast migratory activity, and Rac1, which helps stabilise extended lamellipodial protrusions (Machacek et al., 2009; Mendoza-Naranjo et al., 2012).

Cx26 was found to be slightly elevated in wounds containing uncoated scaffolds but was significantly reduced in Cx43asODN coated scaffolds on days 3 & 5. Elevated Cx26 has been linked to linked hyperproliferative skin conditions and to wounds in which healing is perturbed (Djalilian et al., 2006; Labarthe et al., 1998; Sutcliffe et al., 2015; Wang et al., 2007). Indeed elevated Cx26 has also been found to delay restoration of the epidermal barrier and promote the formation of an inflammatory response (Djalilian et al., 2006). The reduction in Cx26 levels seen in the Cx43asODN coated scaffolds may reflect a reduction in the inflammatory response in these wounds, which was seen as a reduction in the

number of neutrophils in the wound edge dermis and a reduced thickness of the nascent epidermis.

The presence of hair regrowth, scab formation and the ability of scaffolds to mask the wound bed prevented accurate measurements being made from macroscopic evaluations, so the wounds were examined microscopically. Coated scaffolds appeared to act purely as a drug-delivery device while offering little to no structural support to the wound. However, coating scaffolds with Cx43asODN resulted in an almost doubling of wound re-epithelialisation distance at each time point examined compared to scaffolds coated with the sense sequence. Furthermore, the Cx43asODN scaffold-treated wounds had re-epithelialised about 40% further than untreated wounds ($P < 0.01$). This suggests that coating non-cross-linked scaffolds with Cx43asODN actually improved wound healing, unlike our previous studies where bioactivation of cross-linked collagen scaffolds by dipping them in Cx43asOND Pluronic gel appeared to only reduce the negative foreign body side effects of using cross-linked collagen scaffolds (Gilmartin et al., 2013). These results are supported by previous studies, where wound re-epithelialisation was found to be enhanced following Cx43asODN application. This is the first time a similar result has been achieved using a sustained Cx43asODN delivery approach rather than a bolus of drug at the start of the healing process (Mori et al., 2006; Qiu et al., 2003; Wang et al., 2007).

The Cx43asODN significantly reduced Cx43 expression in wound edge keratinocytes at D1, D3 and D5, relative to the control scaffolds, which is likely to enhance their rate of migration. However, it has also been proposed that Cx43 may act as a master regulator with the ability to influence expression of over 300 other genes (Iacobas et al., 2007) so the beneficial effects on wound healing may be through the control of other genes yet to be identified. The finding that Cx43 remained downregulated even at the later time point of D5 indicated that the coating continued to elute Cx43asODN, since the control coated scaffolds had a significantly higher Cx43 expression in wound edge keratinocytes. In our previous study where we bioactivated collagen scaffolds by soaking them in Cx43asODN Pluronic gel, the antisense had long been destroyed by D5 and Cx43 levels were elevated (Gilmartin et al., 2013).

While *in vitro* assays had highlighted the ability of scaffold coatings to elute asODN in a sustained manner, evaluation of treated wounds at D10 and 15 gave a clearer indication of

the long-term biological efficacy of the coatings. At these later time points scaffolds were no longer visible within wounds when they were harvested. This could be due to degradation of the scaffold fibres or the loss of the shrunken scaffolds, which were never integrated into the wound site (Ishaug et al., 1994). The loss of the Tegaderm film securing scaffolds before these time points also adds to this possibility. Wounds that received a Cx43asODN coated scaffold had significantly smaller regions of granulation tissue, the tissue rich in fibroblasts and blood vessels, when compared to all the other treatments. These wounds appeared to be further along in the wound maturation process than the other treatments.

These new coated scaffolds that provide a sustained release of Cx43asODN not only overcome the foreign body reaction caused by scaffolds but also significantly enhance the healing process. These could be particularly effective in treating chronic wounds that significantly overexpress Cx43 (Sutcliffe et al., 2015). This may be particularly applicable to venus leg ulcers where the standard of care is to apply compression bandages which are changed on a weekly basis. The slow release would mean that drug delivery would be sustained for the whole week.

Experimental Details:

Scaffold fabrication

Collagen scaffolds were fabricated by electrospinning acid-soluble bovine collagen (>99% purity, Kensey Nash, PA, USA) blended with poly-ε-caprolactone (>99% purity, Sigma Aldrich, Poole, UK) at a 10:1 weight ratio, respectively. Blended polymers were dissolved in hexafluoropropan-2-ol (HFP, 99% purity, Apollo Scientific, UK) at 10% (wt./v.). The general electrospinning process has been described previously (Torres-Giner et al., 2009). Scaffolds were electrospun at a flow rate of 5 ml/hour, with a needle to collector distance of 130 mm and using an output voltage of 13 kV. 14 ml of polymer solution was spun onto a 9 cm^2 foil sheet to produce scaffolds with an average thickness of 0.4 mm. To generate scaffolds with an average thickness 0.8 mm, 30 ml of polymer solution was electrospun. Uncoated electrospun scaffolds were crossl-inked by immersion in either a high (15% wt./v.) or a low (0.15% wt./v.) concentration of N-(3-Dimethylaminopropyl)-N'-

ethylcarbodiimide (EDC) hydrochloride (99.5% purity, Apollo) in a 1:10 water to acetone solution. Scaffolds were washed for 20 min with sterile PBS, sterilised for 1 h using 70% ethanol, and washed 3 times with sterile PBS. Scaffold discs were then punched out using a 6 mm biopsy punch to match the size and shape of excisional wounds.

Application of polymer coatings containing Cx43 asODN to scaffolds

The rat Cx43asODN sequence 5'-GTA ATT GCG GCA GGA GGA ATT GTT TCT GTC-3'. A non-functional sense (sODN) sequence 5'- GAC AGA AAC AAT TCC TCC TGC CGC AAT TAC-3'. A modified version of the Cx43 asODN sequence had the fluorophores Cy3 and Cy5 conjugated at the 5' and 3' ends, respectively. Either PCL or Poly(D, L-lactice-co-glycolide) (PLGA) was dissolved in dimethyl carbonate at 10% wt./v. The asODN sequences were dissolved in water and mixed with the polymer solutions to either a 100 μM or 300 μM final DNA concentration. The two immiscible layers were processed for 10 seconds using a handheld homogenizer on a medium setting at room temperature to produce an emulsion. After preparing the coating mixture, individual 6 mm collagen scaffolds were dipped for 1 second in the desired polymer-asODN solutions and immediately placed in a tube of liquid nitrogen and lyophilised overnight to remove the solvent from the scaffolds. In some experiments this coating process was repeated 3 times to produce 4 layers of polymer + asODN, or 7 times in the case of 'double coated' scaffolds, which received 4 coating layers of PCL + asODN followed by 4 layers of PLGA + asODN.

Quantification of asODN elution

Three coated scaffolds were immersed in 30 μl of nuclease free water at 37°C. At specified intervals, 1.5 μl of liquid was removed and assayed in a NanoDrop UV spectrophotometer under the ssDNA setting to determine DNA concentration. Scaffolds were placed in a fresh 30 μl of water to compensate for the reduction in volume following water removal for assays. Individual time point elution data was collected to produce both cumulative and daily asODN elution graphs.

Förster Resonance Energy Transfer analysis

The integrity of asODN incorporated into scaffolds was assessed using Förster Resonance Energy Transfer (FRET) imaging. Scaffolds were coated with Cx43 asODN conjugated at either end to fluorophores Cy3 and Cy5. Scaffolds were either left untreated or submerged in 37°C foetal bovine serum (FBS) for up to 7 days. Samples were removed every 24 h then snap frozen in TissueTek O.C.T. medium (Sakura Finetek, UK), and sectioned to a

thickness of 10 μm using a Leica cryostat. Scaffold sections were then washed briefly with PBS and mounted with a size 1 coverslip using Citifluor AF1 mountant (Citfluor Ltd, UK). Samples were imaged using a Leica SP8 confocal microscope using the FRET wizard. Six regions were selected at random for acceptor fluorophore (Cy5) bleaching using a 633 nm laser. A marked increase in Cy3 signal emission at 570 nm post-bleaching was considered to be indicative of FRET activity and was used to calculate a FRET efficiency. Images captured were 8-bit single optical sections with a resolution of 1024 by 1024 pixels. To determine the potency of serum in degrading asODN the wavelength emission spectra of 6 asODN regions per time point were generated by performing xyλ-mode scans on FRET labelled asODN that had been incubated in FBS at 37°C. Individual λ-scans were performed using a 543 nm laser excitation, with 19 equally sized detection steps occurring between the wavelengths of 550 nm to 730 nm. Emission values were output using the LAS AF software.

Surgery

Sprague Dawley rats were reared on site at the BSU and used at 6 weeks old. Rats were anaesthetised using 4% isoflurane, 20% oxygen and 10% nitrous oxide, and maintained using 1.5% isoflurane. Animals were injected subcutaneously with 0.03 mg/ml buprenorphine (Vetergesic) before operation. Rat backs were shaved and covered in a thin layer of Nair® hair removal cream, after which both the cream and hair was removed using a warm moistened gauze pad. Animals were placed on heated mats and four full-thickness excisional 6 mm biopsy punch wounds were made two on each side of the dorsal midline. Scaffold treatments were applied directly to wounds, after which the back was covered with a sheet of Tegaderm™ film. Post-procedure, animals were kept in a heated chamber and monitored for recovery.

Harvesting wounds

Animals were culled by cervical dislocation at 1, 3, 5, 10 or 15 days post wounding (N=8 per time point). Wounds were macroscopically imaged with a Leica MZ8 dissection microscope and then excised and fixed in 4% paraformaldehyde for 24 h at 4°C and transferred to 20% sucrose overnight, washed in PBS then bisected. Half of each wound was snap frozen in O.C.T. medium, then sectioned using a cryostat at a thickness of either 5 μm (for H&E staining) or 10 μm (for immunofluorescence staining).

Haematoxylin and eosin staining

Frozen tissue sections were thawed then covered completely in tap water for 5 min at room temperature. Slides were submerged in Harris' haematoxylin solution for 30 seconds

followed by washing in running tap water for 5 min. Background staining was reduced by dipping the slides in 1% acid alcohol (1% glacial hydrochloric acid, 70% ethanol, 29% distilled water) for 3 seconds, followed by running tap water for a further 5 min. Samples were then submerged for 15 seconds in eosin B solution, followed by 5 seconds in a tap water, then 70% ethanol for 2 min, 100% ethanol for 2 min and a second 100% ethanol for a further 2 min, to dehydrate the sections followed by 2 X xylene for 5 min. Slides were then mounted in a xylene based DPX mountant and coversliped.

Immunofluorescence staining

Tissue sections were permeabilised in cold acetone for 5 min and then blocked using a 0.1 M lysine PBS solution containing 0.1% Triton-X-100. Sections were stained for 1 h using a rabbit polyclonal antibody to Cx43 (1:2000 dilution, C6219, Sigma Aldrich UK) or Cx26 Cx26 (1:200 dilution, (Diez et al., 1999). Sections were then stained using a goat anti-rabbit Alexa 488 secondary antibody (A11008, Invitrogen UK) at a 1:400 dilution for 1 h. Tissue was counterstained using Hoechst solution (both Hoechst 33528 and Hoechst 33342 dyes at 1:50,000 dilution, Sigma Aldrich UK). Slides were mounted in citifluor and coverslipped.

Epidermal measurements

H&E stained sections were examined using a Leica DMLB light microscope and images were captured at either 10 X or 20 X magnification. Epidermal thickness was determined by measuring the thickest point along the basal to spinous layer axis within the end 100 µm of nascent epidermis using ImageJ. The length of nascent epidermis outgrowing from the wound margin was measured at either side of the wound using ImageJ and averaged to return a re-epithelialisation distance measurement for each sample.

Polymorphonuclear cell quantification

H&E stained tissue sections were examined using a light microscope and polymorphonuclear cells (PMNs) were identified 3 fields of view from the wound edge in the dermis using a 40 X objective. Individual images of this region for each sample were then captured using a 20 X objective. The numbers of PMNs in this area was quantified manually with assistance of a counter tool in ImageJ.

Measurement of granulation tissue area smooth muscle actin area

Rat wounds harvested at D10 and D15 were H&E stained and imaged with a Zeiss Axio Scan.Z1 automated slide scanner. Brightfield images were captured using a 20 X objective

then automatically stitched together to form a montage and quantified for granulation tissue area using ImageJ.

Confocal microscopy and image analysis

Single optical section images of Cx43 or Cx26 immunostained tissue sections were acquired using a Leica SP2 confocal microscope with a 40 X oil objective. 8-bit images were acquired 1024 by 1024 pixels. Image acquisition settings remained identical between each treatment in order to allow comparisons to be made during image analysis. Connexin protein expression was quantified by counting positive pixels on binary images of wound edges with ImageJ software using the method outlined in a study by (Wang et al., 2007). Images from each experiment were identically thresholded. Only the number of connexin positive pixels contained within the end 150 μm of the nascent epidermis was assessed in order to gauge only protein expression at the epidermal wound edge. Connexin levels were expressed per square micron of epidermis to compensate for variations in epidermal thickness between samples. In order to account for variations in connexin levels between individual animals, wound edge expression was normalised to connexin levels at a distal site away from the wound edge and expressed as a percentage change from distal levels. In the case of Cx26 stained tissue, distal levels were extremely low, to the extent that small fluctuations between samples could result in large differences between values. For this reason, Cx26 distal levels were averaged and these values were used to calculate the change in wound edge Cx26 expression.

Statistical analysis

All data amenable to statistical analysis was subjected to Kolmogorov-Smirnov tests to ascertain normality. Normally distributed data was then subjected to parametric statistical tests. Other data or multiple comparisons was subjected to a one-way ANOVA test followed by a Tukey's post-hoc test to investigate individual statistical significance differences. GraphPad Prism 5.0 software was used to perform all statistical analyses.

Figure legends:

Figure 1. Cx43 asODN elution from differing combinations of scaffold coatings. (A) Electrospun collagen scaffolds were dipped in an emulsion of 100 μM Cx43 asODN and either 10% or 15% PLGA and immediately subject to freezing and lyophilisation. (B) Cumulative Cx43 asODN elution from scaffolds was quantified in water at 37 °C over 4 days. (C) Schematic illustrating the procedure used to create scaffolds with multiple coating layers. (D) Elution profile from scaffolds subject to one round of processing. (E)

Elution profile from scaffolds subject to four rounds of processing. The average of three samples was recorded for all elution measurements and error bars represent SEM.

Figure 2. Analysis of asODN degradation in PCL+PLGA coated scaffolds. (A) Simplified diagram of asODN coated scaffold illustrating the stochastic dispersion of asODN clusters across the scaffold as well as the site at which images were captured in (D). (B) Scaffolds were submerged in FBS for up to 7 days, after which they were sectioned and acceptor bleached using a confocal 633 nm wavelength laser. FRET efficiency was calculated as a percentage increase in donor fluorescence intensity after acceptor bleaching relative to before acceptor bleaching. A total of 6 regions were quantified per time point, graph data = means + SEM error bars. (C) xyλ scans were performed on a 300 μM asODN solution either treated or untreated with FBS for 8 h to test the potency of the FBS as a nuclease effective against asODN. The mean fluorescence intensity values detected at 19 steps between 550 nm and 730 nm following excitation with a 533 nm laser were plotted. Six regions were assessed to generate averages. (D) A typical confocal image of a scaffold section following immersion in FBS used to generate the FRET efficiencies plotted in (B). Images show labelled asODN clusters both before and after Cy5 bleaching. Scale bar = 20 μm.

Figure 3. Macroscopic wound evaluation following coated scaffold placement. (A) Full thickness rat wounds were treated with one of a number of different collagen scaffolds or left untreated. (B) Animals were culled at either 1, 3 or 5 days after wounding and the wounds macroscopically imaged. Scale bar = 1 mm.

Figure 4. Day 1 full thickness wound healing following application of the various scaffolds. (A) Panel showing representative H&E and immunofluorescent staining (Cx43 or Cx26 in green; Hoechst in blue) images from wounds subject to the indicated treatments. Re-epithelialisation is marked by yellow dotted lines on the H&E stains. Epithelium is marked by white dotted lines on the immunofluorescent stains. (B) Wound re-epithelialisation distances. (C) Percentage change in epidermal wound edge Cx43 normalized to regions of distal epidermis. (D) Percentage change in epidermal wound edge Cx26 normalized to regions of distal epidermis. Plotted as means + SEM error bars. Eight rat wounds per condition were assessed. Dunnett's test conducted against the untreated control (* $p < 0.05$, ** $p < 0.01$, *** $p < 0.001$). Scale bar = 100 μm.

Figure 5. Day 3 full thickness wound healing following application of the various scaffolds. (A) Panel showing representative H&E and immunofluorescent staining (Cx43 or Cx26 in green; Hoechst in blue) images from wounds subject to the indicated treatments. Re-epithelialisation is marked by yellow dotted lines on the H&E stains. Epithelium is marked by white dotted lines on the immunofluorescent stains. (B) Wound re-epithelialisation distances. (C) Percentage change in epidermal wound edge Cx43 normalized to regions of distal epidermis. (D) Percentage change in epidermal wound edge Cx26 normalized to regions of distal epidermis. Plotted as means + SEM error bars. Eight rat wounds per condition were assessed. Dunnett's test conducted against the untreated control (* $p < 0.05$, ** $p < 0.01$, *** $p < 0.001$). Scale bar = 100 μm.

Figure 6. Day 5 full thickness wound healing following application of the various scaffolds. (A) Panel showing representative H&E and immunofluorescent staining (Cx43 or Cx26 in green; Hoechst in blue) images from wounds subject to the indicated treatments. Re-epithelialisation is marked by yellow dotted lines on the H&E stains. Epithelium is marked by white dotted lines on the immunofluorescent stains. (B) Wound re-epithelialisation distances. (C) Percentage change in epidermal wound edge Cx43 normalized to regions of distal epidermis. (D) Percentage change in epidermal wound edge Cx26 normalized to regions of distal epidermis. Plotted as means + SEM error bars. Eight rat wounds per condition were assessed. Dunnett's test conducted against the untreated control (* $p < 0.05$, ** $p < 0.01$, *** $p < 0.001$). Scale bar = 100 μm.

Figure 7. The effect of scaffold application on epidermal thickening and dermal infiltration of polymorphonuclear cells. (A) Full thickness wounds treated with different types of scaffolds were measured for epithelial thickness within the end 150 μm of the nascent tip of epidermis. Measurements were recorded across n = 8 samples per timepoint. (B) Full-thickness wounds that received a scaffold treatment were assessed for polymorphonuclear cell invasion into the lower dermis 700 μm away from the wound edge as indicated in the topleft of diagram. E = epidermis, D = dermis, PC = panniculus carnosus, WE = wound edge. High-power typical images of the dermal region are also shown for each scaffold treatment. The typical images shown are of the unwounded dermis distal to day 3 wounds. Scale bar = 50 μm. (C) Quantification of polymorphonuclear cells for each treatment. Plotted as average values of n = 5 samples per timepoint. Error bars represent SEM. Dunnett's test conducted against the untreated control (* $p < 0.05$, ** $p < 0.01$, *** $p < 0.001$).

Figure 8. Long-term full thickness wound healing following application of the various scaffolds. (A) Panel showing representative H&E images from day 10 wounds subject to the indicated treatments. Granulation tissue area is marked by white dotted lines. (B-C) Quantification of granulation tissue area on days 10 and 15. Plotted as average values of n = 8 samples per timepoint. Error bars represent SEM. Dunnett's test conducted against the untreated control (* $p < 0.05$, ** $p < 0.01$, *** $p < 0.001$). Scale bar = 100 μm.

References:

Acharya, G., Lee, C. H. and Lee, Y. (2012). Optimization of cardiovascular stent against restenosis: factorial design-based statistical analysis of polymer coating conditions. *PLoS One* **7**, e43100.

Atiyeh, B. S. and Costagliola, M. (2007). Cultured epithelial autograft (CEA) in burn treatment: three decades later. *Burns* **33**, 405-13.

Bioscience, F. Orcel Product http://www.forticellbioscience.com/orcel.html.

Chen, D. W., Liao, J. Y., Liu, S. J. and Chan, E. C. (2012). Novel biodegradable sandwich-structured nanofibrous drug-eluting membranes for repair of infected wounds: an in vitro and in vivo study. *Int J Nanomedicine* **7**, 763-71.

Cronin, M., Anderson, P. N., Green, C. R. and Becker, D. L. (2006). Antisense delivery and protein knockdown within the intact central nervous system. *Front Biosci* **11**, 2967-75.

Djalilian, A. R., McGaughey, D., Patel, S., Seo, E. Y., Yang, C., Cheng, J., Tomic, M., Sinha, S., Ishida-Yamamoto, A. and Segre, J. A. (2006). Connexin 26 regulates epidermal barrier and wound remodeling and promotes psoriasiform response. *J Clin Invest* **116**, 1243-53.

Farag, Y. M. and Gaballa, M. R. (2011). Diabesity: an overview of a rising epidemic. *Nephrol Dial Transplant* **26**, 28-35.

Gilmartin, D. J., Alexaline, M. M., Thrasivoulou, C., Phillips, A. R., Jayasinghe, S. N. and Becker, D. L. (2013). Integration of scaffolds into full-thickness skin wounds: the connexin response. *Adv Healthc Mater* **2**, 1151-60.

Iacobas, D. A., Iacobas, S. and Spray, D. C. (2007). Connexin-dependent transcellular transcriptomic networks in mouse brain. *Prog Biophys Mol Biol* **94**, 169-85.

Ishaug, S. L., Yaszemski, M. J., Bizios, R. and Mikos, A. G. (1994). Osteoblast function on synthetic biodegradable polymers. *J Biomed Mater Res* **28**, 1445-53.

Khan, A., Benboubetra, M., Sayyed, P. Z., Ng, K. W., Fox, S., Beck, G., Benter, I. F. and Akhtar, S. (2004). Sustained polymeric delivery of gene silencing antisense ODNs, siRNA, DNAzymes and ribozymes: in vitro and in vivo studies. *J Drug Target* **12**, 393-404.

Kipshidze, N., Tsapenko, M., Iversen, P. and Burger, D. (2005). Antisense therapy for restenosis following percutaneous coronary intervention. *Expert Opin Biol Ther* **5**, 79-89.

Krucoff, M. W., Kereiakes, D. J., Petersen, J. L., Mehran, R., Hasselblad, V., Lansky, A. J., Fitzgerald, P. J., Garg, J., Turco, M. A., Simonton, C. A., 3rd et al. (2008). A novel bioresorbable polymer paclitaxel-eluting stent for the treatment of single and multivessel coronary disease: primary results of the COSTAR (Cobalt Chromium Stent With Antiproliferative for Restenosis) II study. *J Am Coll Cardiol* **51**, 1543-52.

Labarthe, M. P., Bosco, D., Saurat, J. H., Meda, P. and Salomon, D. (1998). Upregulation of connexin 26 between keratinocytes of psoriatic lesions. *J Invest Dermatol* **111**, 72-6.

Lai, X. J., Ye, S. Q., Zheng, L., Li, L., Liu, Q. R., Yu, S. B., Pang, Y., Jin, S., Li, Q., Yu, A. C. et al. (2014). Selective 14-3-3gamma induction quenches p-beta-catenin Ser37/Bax-enhanced cell death in cerebral cortical neurons during ischemia. *Cell Death Dis* **5**, e1184.

Machacek, M., Hodgson, L., Welch, C., Elliott, H., Pertz, O., Nalbant, P., Abell, A., Johnson, G. L., Hahn, K. M. and Danuser, G. (2009). Coordination of Rho GTPase activities during cell protrusion. *Nature* **461**, 99-103.

Makadia, H. K. and Siegel, S. J. (2011). Poly Lactic-co-Glycolic Acid (PLGA) as Biodegradable Controlled Drug Delivery Carrier. *Polymers (Basel)* **3**, 1377-1397.

Mehilli, J., Kastrati, A., Wessely, R., Dibra, A., Hausleiter, J., Jaschke, B., Dirschinger, J., Schomig, A., Intracoronary, S. and Angiographic Restenosis--Test Equivalence Between 2 Drug-Eluting Stents Trial, I. (2006). Randomized trial of a nonpolymer-based rapamycin-eluting stent versus a polymer-based paclitaxel-eluting stent for the reduction of late lumen loss. *Circulation* **113**, 273-9.

Mendoza-Naranjo, A., Cormie, P., Serrano, A. E., Hu, R., O'Neill, S., Wang, C. M., Thrasivoulou, C., Power, K. T., White, A., Serena, T. et al. (2012). Targeting Cx43 and N-cadherin, which are abnormally upregulated in venous leg ulcers, influences migration, adhesion and activation of Rho GTPases. *PLoS One* **7**, e37374.

Mori, R., Power, K. T., Wang, C. M., Martin, P. and Becker, D. L. (2006). Acute downregulation of connexin43 at wound sites leads to a reduced inflammatory response, enhanced keratinocyte proliferation and wound fibroblast migration. *J Cell Sci* **119**, 5193-203.

Mustoe, T. (2004). Understanding chronic wounds: a unifying hypothesis on their pathogenesis and implications for therapy. *Am J Surg* **187**, 65S-70S.

Nunan, R., Harding, K. G. and Martin, P. (2014). Clinical challenges of chronic wounds: searching for an optimal animal model to recapitulate their complexity. *Dis Model Mech* **7**, 1205-13.

Qiu, C., Coutinho, P., Frank, S., Franke, S., Law, L. Y., Martin, P., Green, C. R. and Becker, D. L. (2003). Targeting connexin43 expression accelerates the rate of wound repair. *Curr Biol* **13**, 1697-703.

Rupenthal, I. G., CR ; Alany, RG. (2012). Evaluation of Fluorescence Resonance Energy Transfer approaches as a tool to quantify the stability of antisense oligodeoxynucleotides. *Current Pharmaceutical Analysis* **8**, 20-27.

Schofer, J., Schluter, M., Gershlick, A. H., Wijns, W., Garcia, E., Schampaert, E., Breithardt, G. and Investigators, E. S. (2003). Sirolimus-eluting stents for treatment of patients with long atherosclerotic lesions in small coronary arteries: double-blind, randomised controlled trial (E-SIRIUS). *Lancet* **362**, 1093-9.

Sen, C. K., Gordillo, G. M., Roy, S., Kirsner, R., Lambert, L., Hunt, T. K., Gottrup, F., Gurtner, G. C. and Longaker, M. T. (2009). Human skin wounds: a major and snowballing threat to public health and the economy. *Wound Repair Regen* **17**, 763-71.

Shive, M. S. and Anderson, J. M. (1997). Biodegradation and biocompatibility of PLA and PLGA microspheres. *Adv Drug Deliv Rev* **28**, 5-24.

Sutcliffe, J. E., Chin, K. Y., Thrasivoulou, C., Serena, T. E., O'Neil, S., Hu, R., White, A. M., Madden, L., Richards, T., Phillips, A. R. et al. (2015). Abnormal connexin expression in human chronic wounds. *Br J Dermatol*.

Tarvainen, T., Karjalainen, T., Malin, M., Perakorpi, K., Tuominen, J., Seppala, J. and Jarvinen, K. (2002). Drug release profiles from and degradation of a novel biodegradable polymer, 2,2-bis(2-oxazoline) linked poly(epsilon -caprolactone). *Eur J Pharm Sci* **16**, 323-31.

Torres-Giner, S., Gimeno-Alcaniz, J. V., Ocio, M. J. and Lagaron, J. M. (2009). Comparative performance of electrospun collagen nanofibers cross-linked by means of different methods. *ACS Appl Mater Interfaces* **1**, 218-23.

Wang, C. M., Lincoln, J., Cook, J. E. and Becker, D. L. (2007). Abnormal connexin expression underlies delayed wound healing in diabetic skin. *Diabetes* **56**, 2809-17.

Wieneke, H., Dirsch, O., Sawitowski, T., Gu, Y. L., Brauer, H., Dahmen, U., Fischer, A., Wnendt, S. and Erbel, R. (2003). Synergistic effects of a novel nanoporous stent coating and tacrolimus on intima proliferation in rabbits. *Catheter Cardiovasc Interv* **60**, 399-407.

Windecker, S., Serruys, P. W., Wandel, S., Buszman, P., Trznadel, S., Linke, A., Lenk, K., Ischinger, T., Klauss, V., Eberli, F. et al. (2008). Biolimus-eluting stent with biodegradable polymer versus sirolimus-eluting stent with durable polymer for coronary revascularisation (LEADERS): a randomised non-inferiority trial. *Lancet* **372**, 1163-73.

Zhong, S. P., Zhang, Y. Z. and Lim, C. T. (2010). Tissue scaffolds for skin wound healing and dermal reconstruction. *Wiley Interdiscip Rev Nanomed Nanobiotechnol* **2**, 510-25.

Figure 1. Cx43 asODN elution from differing combinations of scaffold coatings. (A) Electrospun collagen scaffolds were dipped in an emulsion of 100 μM Cx43 asODN and either 10% or 15% PLGA and immediately subject to freezing and lyophilisation. (B) Cumulative Cx43 asODN elution from scaffolds was quantified in water at 37 °C over 4 days. (C) Schematic illustrating the procedure used to create scaffolds with multiple coating layers. (D) Elution profile from scaffolds subject to one round of processing. (E) Elution profile from scaffolds subject to four rounds of processing. The average of three samples was recorded for all elution measurements and error bars represent SEM.

Figure 2. Analysis of asODN degradation in PCL+PLGA coated scaffolds. (A) Simplified diagram of asODN coated scaffold illustrating the stochastic dispersion of asODN clusters across the scaffold as well as the site at which images were captured in (D). (B) Scaffolds were submerged in FBS for up to 7 days, after which they were sectioned and acceptor bleached using a confocal 633 nm wavelength laser. FRET efficiency was calculated as a percentage increase in donor fluorescence intensity after acceptor bleaching relative to before acceptor bleaching. A total of 6 regions were quantified per time point, graph data = means + SEM error bars. (C) xyλ scans were performed on a 300 μM asODN solution either treated or untreated with FBS for 8 h to test the potency of the FBS as a nuclease effective against asODN. The mean fluorescence intensity values detected at 19 steps between 550 nm and 730 nm following excitation with a 533 nm laser were plotted. Six regions were assessed to generate averages. (D) A typical confocal image of a scaffold section following immersion in FBS used to generate the FRET efficiencies plotted in (B). Images show labelled asODN clusters both before and after Cy5 bleaching. Scale bar = 20 μm.

Figure 3. Macroscopic wound evaluation following coated scaffold placement. (A) Full thickness rat wounds were treated with one of a number of different collagen scaffolds or left untreated. (B) Animals were culled at either 1, 3 or 5 days after wounding and the wounds macroscopically imaged. Scale bar = 1 mm.

Figure 4. Day 1 full thickness wound healing following application of the various scaffolds. (A) Panel showing representative H&E and immunofluorescent staining (Cx43 or Cx26 in green; Hoechst in blue) images from wounds subject to the indicated treatments. Re-epithelialisation is marked by yellow dotted lines on the H&E stains. Epithelium is marked by white dotted lines on the immunofluorescent stains. (B) Wound re-epithelialisation distances. (C) Percentage change in epidermal wound edge Cx43 normalized to regions of distal epidermis. (D) Percentage change in epidermal wound edge Cx26 normalized to regions of distal epidermis. Plotted as means + SEM error bars. Eight rat wounds per condition were assessed. Dunnett's test conducted against the untreated control (* $p < 0.05$, ** $p < 0.01$, *** $p < 0.001$). Scale bar = 100 μm.

Figure 5. Day 3 full thickness wound healing following application of the various scaffolds. (A) Panel showing representative H&E and immunofluorescent staining (Cx43 or Cx26 in green; Hoechst in blue) images from wounds subject to the indicated treatments. Re-epithelialisation is marked by yellow dotted lines on the H&E stains. Epithelium is marked by white dotted lines on the immunofluorescent stains. (B) Wound re-epithelialisation distances. (C) Percentage change in epidermal wound edge Cx43 normalized to regions of distal epidermis. (D) Percentage change in epidermal wound edge Cx26 normalized to regions of distal epidermis. Plotted as means + SEM error bars. Eight rat wounds per condition were assessed. Dunnett's test conducted against the untreated control (* $p < 0.05$, ** $p < 0.01$, *** $p < 0.001$). Scale bar = 100 μm.

Figure 6. Day 5 full thickness wound healing following application of the various scaffolds. (A) Panel showing representative H&E and immunofluorescent staining (Cx43 or Cx26 in green; Hoechst in blue) images from wounds subject to the indicated treatments. Re-epithelialisation is marked by yellow dotted lines on the H&E stains. Epithelium is marked by white dotted lines on the immunofluorescent stains. (B) Wound re-epithelialisation distances. (C) Percentage change in epidermal wound edge Cx43 normalized to regions of distal epidermis. (D) Percentage change in epidermal wound edge Cx26 normalized to regions of distal epidermis. Plotted as means + SEM error bars. Eight rat wounds per condition were

assessed. Dunnett's test conducted against the untreated control (* $p < 0.05$, ** $p < 0.01$, *** $p < 0.001$). Scale bar = 100 μm.

Figure 7. The effect of scaffold application on epidermal thickening and dermal infiltration of polymorphonuclear cells. (A) Full thickness wounds treated with different types of scaffolds were measured for epithelial thickness within the end 150 μm of the nascent tip of epidermis. Measurements were recorded across n = 8 samples per timepoint. (B) Full-thickness wounds that received a scaffold treatment were assessed for polymorphonuclear cell invasion into the lower dermis 700 μm away from the wound edge as indicated in the topleft of diagram. E = epidermis, D = dermis, PC = panniculus carnosus, WE = wound edge. High-power typical images of the dermal region are also shown for each scaffold treatment. The typical images shown are of the unwounded dermis distal to day 3 wounds. Scale bar = 50 μm. (C) Quantification of polymorphonuclear cells for each treatment. Plotted as average values of n = 5 samples per timepoint. Error bars represent SEM. Dunnett's test conducted against the untreated control (* $p < 0.05$, ** $p < 0.01$, *** $p < 0.001$).

Figure 8. Long-term full thickness wound healing following application of the various scaffolds. (A) Panel showing representative H&E images from day 10 wounds subject to the indicated treatments. Granulation tissue area is marked by white dotted lines. (B-C) Quantification of granulation tissue area on days 10 and 15. Plotted as average values of n = 8 samples per timepoint. Error bars represent SEM. Dunnett's test conducted against the untreated control (* $p < 0.05$, ** $p < 0.01$, *** $p < 0.001$). Scale bar = 100 μm.

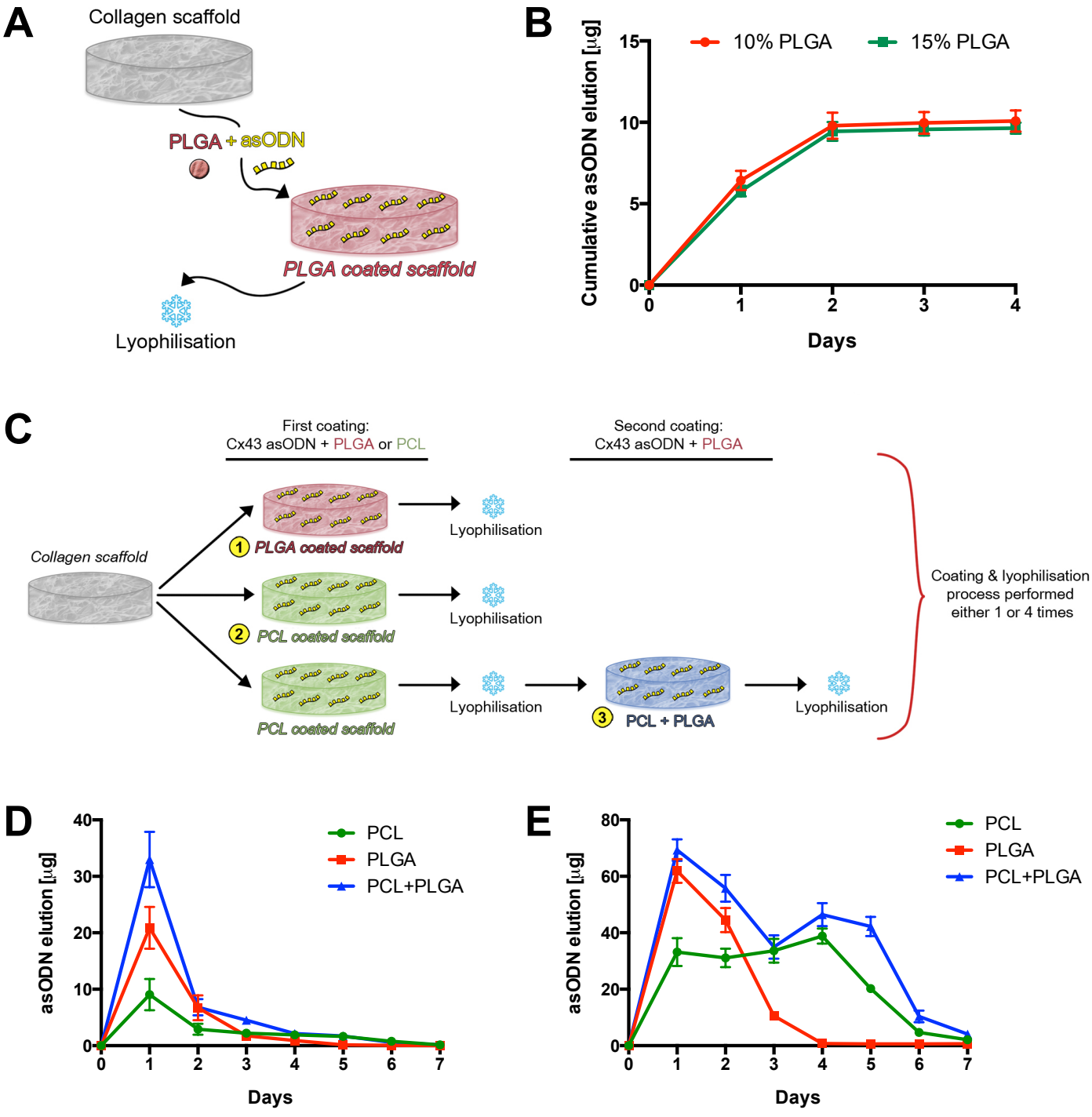
A
Collagen scaffold
PLGA + asODN
PLGA coated scaffold
Lyophilisation
B
10% PLGA
15% PLGA
Cumulative asODN elution [µg]
Days
C
First coating:
Cx43 asODN + PLGA or PCL
Second coating:
Cx43 asODN + PLGA
Collagen scaffold
1 PLGA coated scaffold
2 PCL coated scaffold
PCL coated scaffold
Lyophilisation
3 PCL + PLGA
Coating & lyophilisation process performed either 1 or 4 times
D
PCL
PLGA
PCL+PLGA
asODN elution [µg]
Days
E
PCL
PLGA
PCL+PLGA
asODN elution [µg]
Days

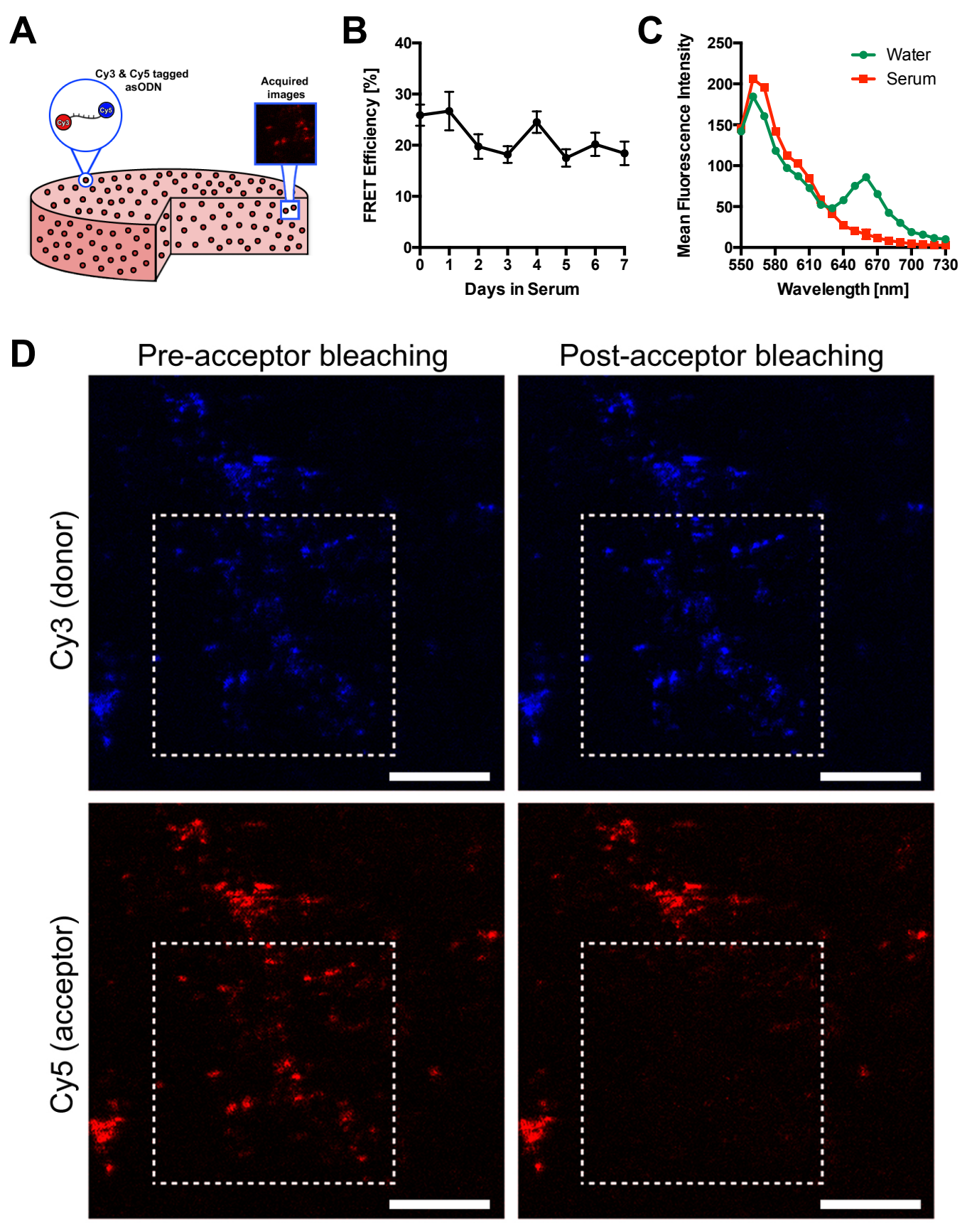
A
Cy3 & Cy5 tagged asODN
Cy3
Cy5
Acquired images
B
FRET Efficiency [%]
40
30
20
10
0
0 1 2 3 4 5 6 7
Days in Serum
C
Mean Fluorescence Intensity
250
200
150
100
50
0
550 580 610 640 670 700 730
Wavelength [nm]
Water
Serum
D
Pre-acceptor bleaching
Post-acceptor bleaching
Cy3 (donor)
Cy5 (acceptor)

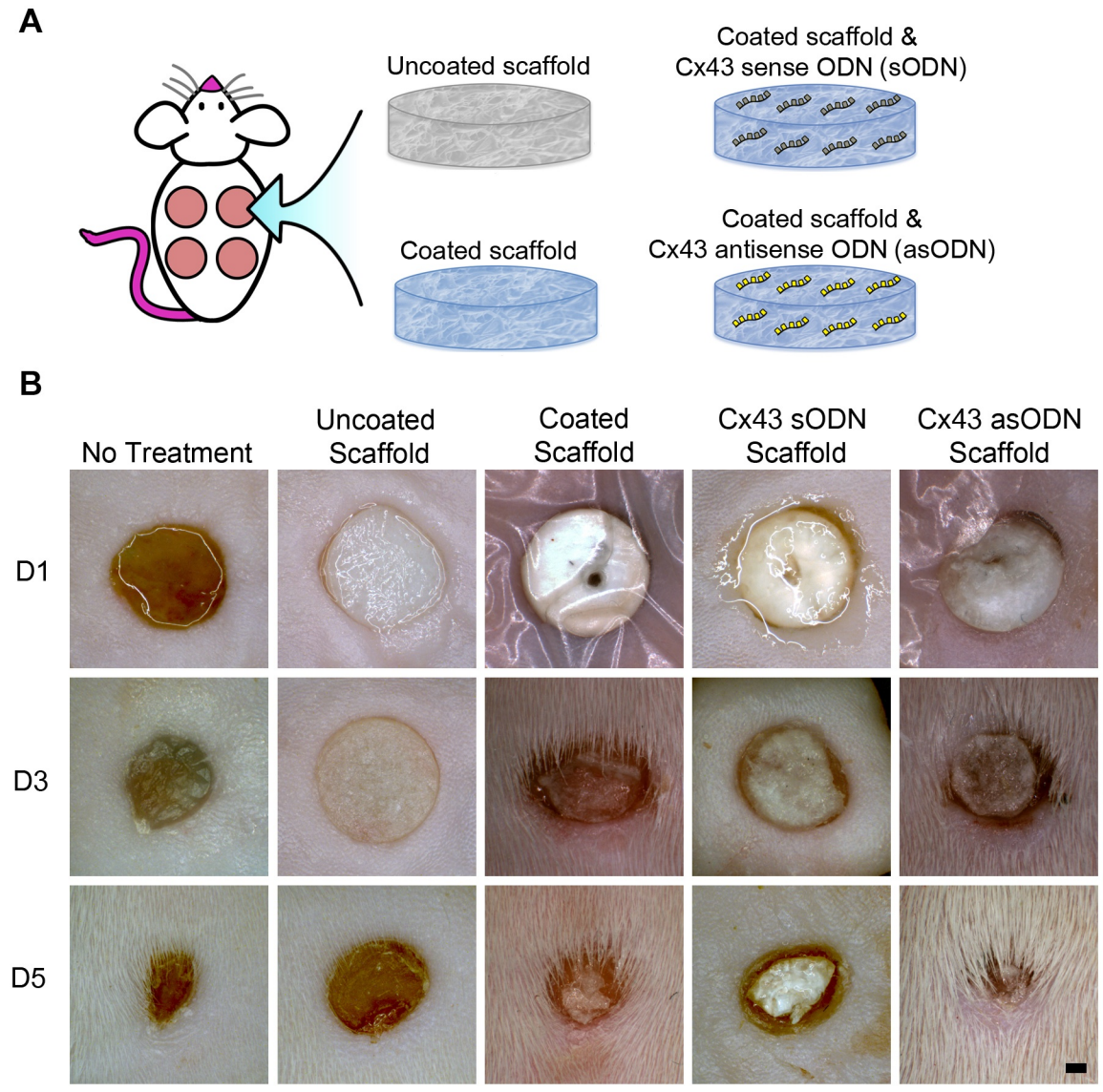
A
Uncoated scaffold
Coated scaffold & Cx43 sense ODN (sODN)
Coated scaffold
Coated scaffold & Cx43 antisense ODN (asODN)
B
No Treatment
Uncoated Scaffold
Coated Scaffold
Cx43 sODN Scaffold
Cx43 asODN Scaffold
D1
D3
D5

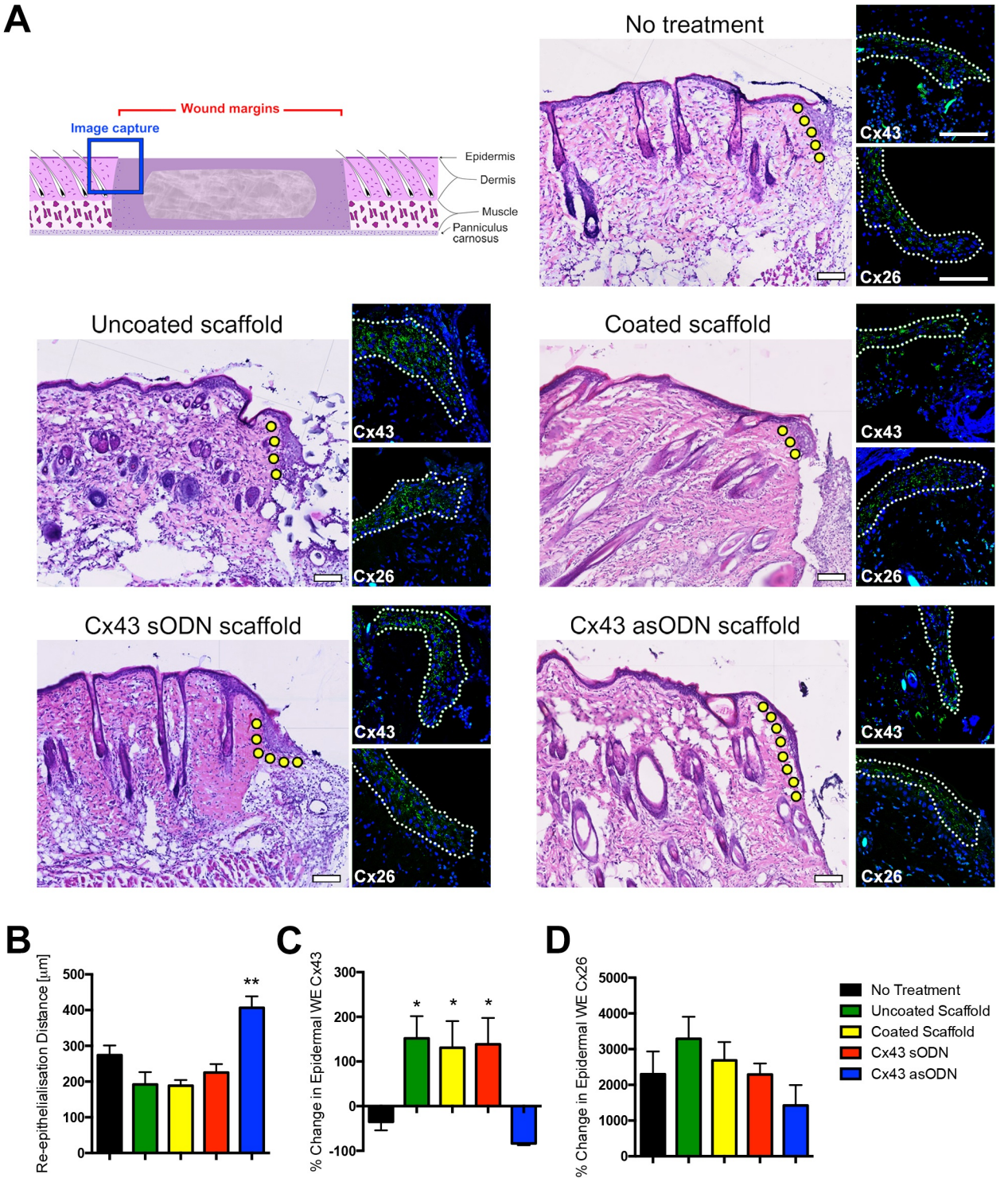
A
Wound margins
Image capture
Epidermis
Dermis
Muscle
Panniculus carnosus
No treatment
Cx43
Cx26
Uncoated scaffold
Coated scaffold
Cx43 sODN scaffold
Cx43 asODN scaffold
B
Re-epithelialisation Distance [μm]
C
% Change in Epidermal WE Cx43
D
% Change in Epidermal WE Cx26
No Treatment
Uncoated Scaffold
Coated Scaffold
Cx43 sODN
Cx43 asODN

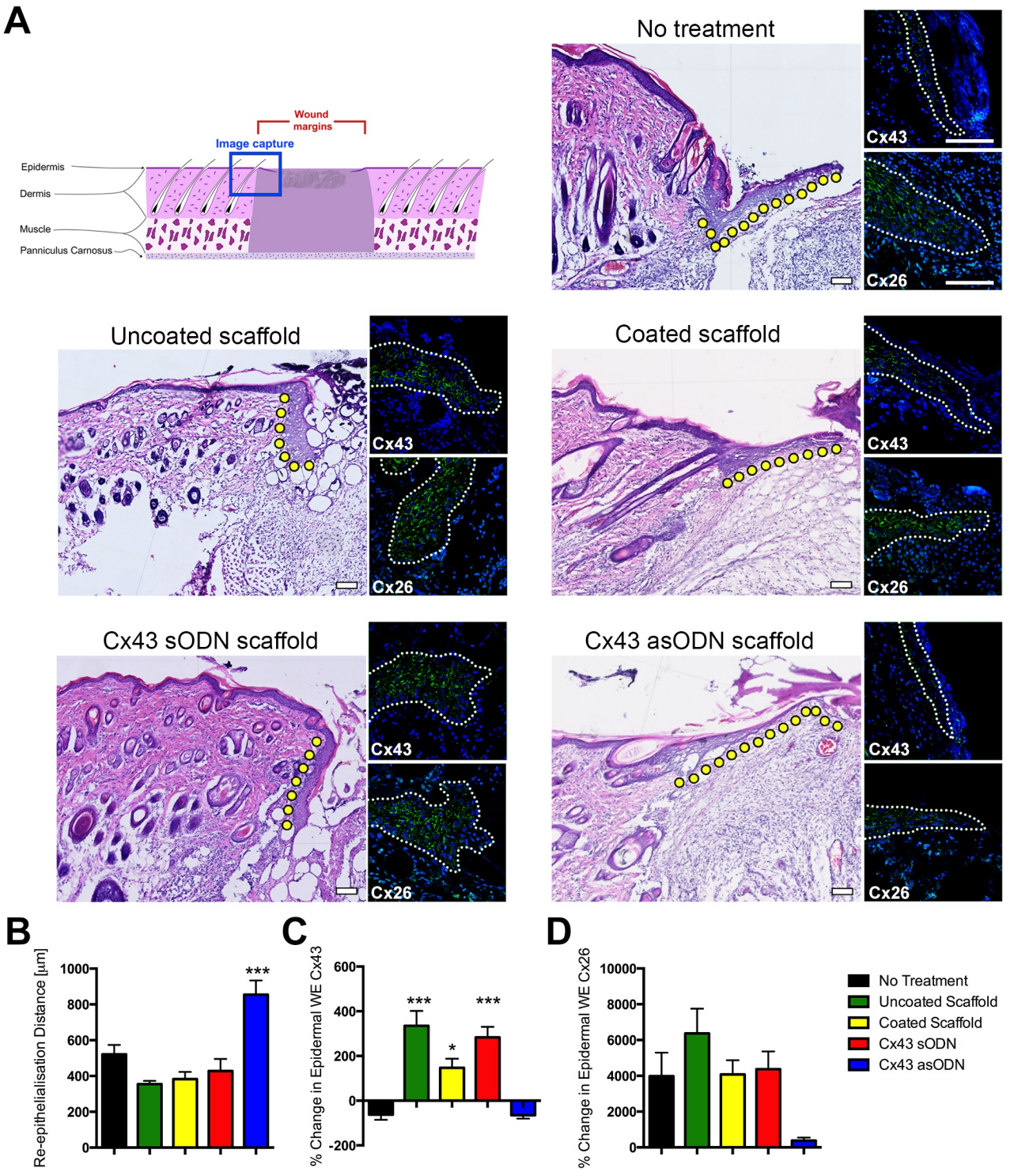
A
No treatment
Wound margins
Image capture
Epidermis
Dermis
Muscle
Panniculus Carnosus
Cx43
Cx26
Uncoated scaffold
Coated scaffold
Cx43 sODN scaffold
Cx43 asODN scaffold
B
Re-epithelialisation Distance [µm]
1000
800
600
400
200
0
***
C
% Change in Epidermal WE Cx43
600
400
200
0
-200
***
*
***
D
% Change in Epidermal WE Cx26
10000
8000
6000
4000
2000
0
No Treatment
Uncoated Scaffold
Coated Scaffold
Cx43 sODN
Cx43 asODN

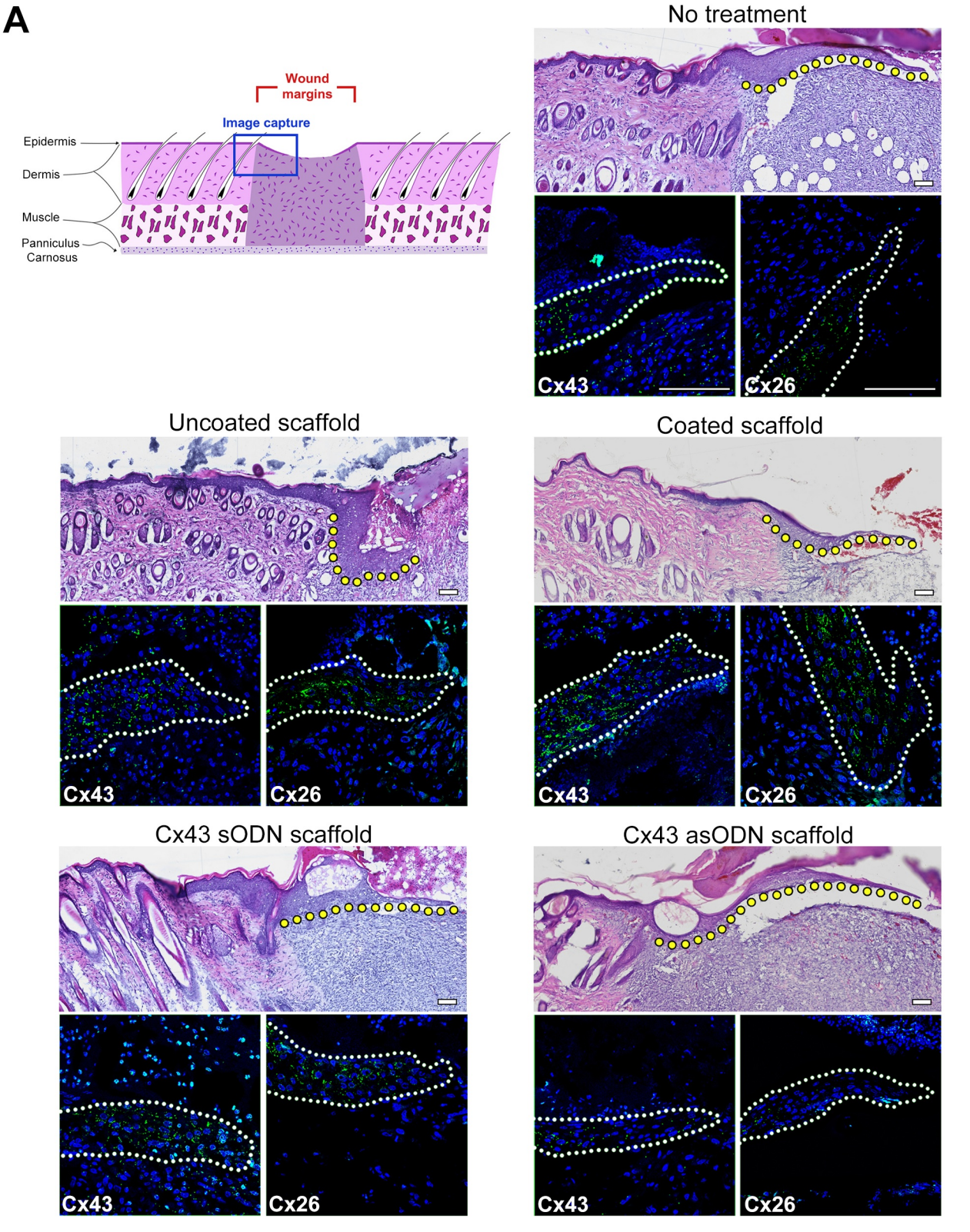
A
Wound margins
Image capture
Epidermis
Dermis
Muscle
Panniculus Carnosus
No treatment
Cx43
Cx26
Uncoated scaffold
Cx43
Cx26
Coated scaffold
Cx43
Cx26
Cx43 sODN scaffold
Cx43
Cx26
Cx43 asODN scaffold
Cx43
Cx26
B
Re-epithelialisation Distance [µm]
2000
1500
1000
500
0
**
C
% Change in Epidermal WE Cx43
400
300
200
100
0
-100
*
**
D
% Change in Epidermal WE Cx26
800
600
400
200
0
-200
No Treatment
Uncoated Scaffold
Coated Scaffold
Cx43 sODN
Cx43 asODN

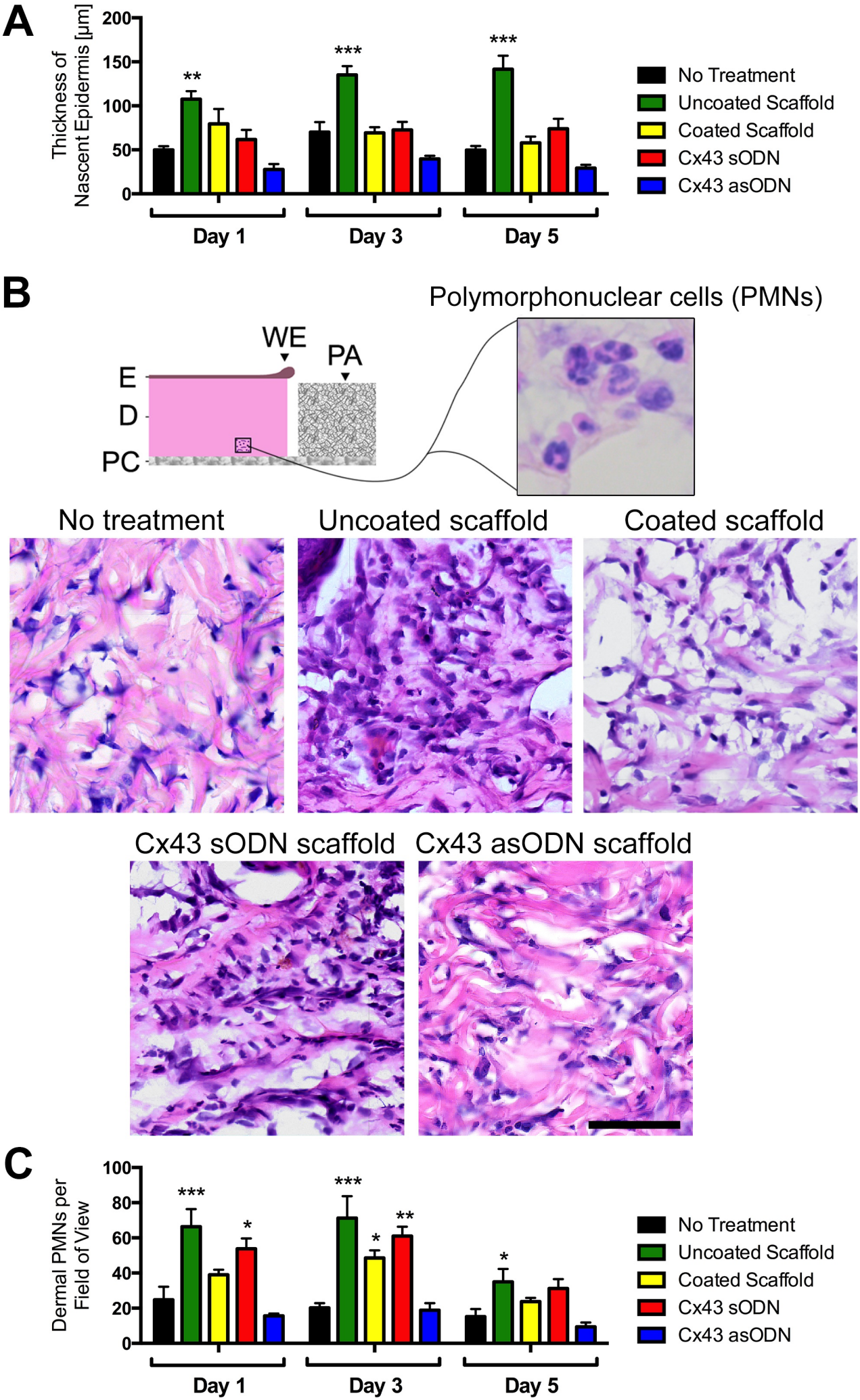
A
Thickness of Nascent Epidermis [µm]
200
150
100
50
0
**
***
***
Day 1
Day 3
Day 5
No Treatment
Uncoated Scaffold
Coated Scaffold
Cx43 sODN
Cx43 asODN
B
Polymorphonuclear cells (PMNs)
WE
PA
E
D
PC
No treatment
Uncoated scaffold
Coated scaffold
Cx43 sODN scaffold
Cx43 asODN scaffold
C
Dermal PMNs per Field of View
100
80
60
40
20
0
***
*
***
*
**
*
Day 1
Day 3
Day 5
No Treatment
Uncoated Scaffold
Coated Scaffold
Cx43 sODN
Cx43 asODN

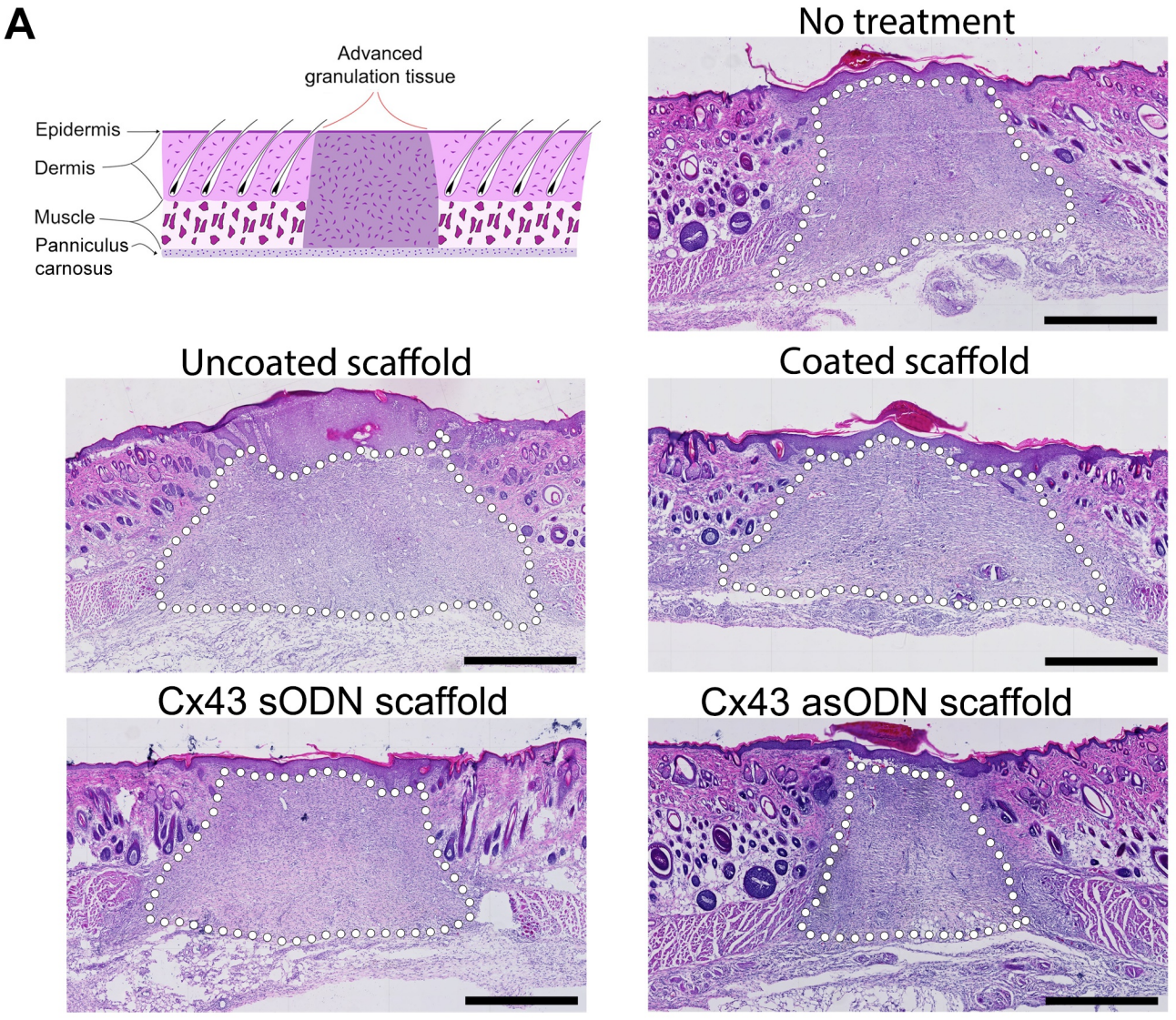
A
Advanced granulation tissue
Epidermis
Dermis
Muscle
Panniculus carnosus
No treatment
Uncoated scaffold
Coated scaffold
Cx43 sODN scaffold
Cx43 asODN scaffold

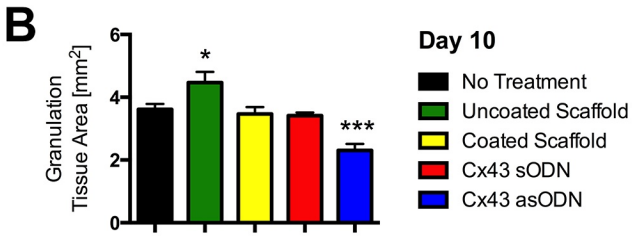
B
Granulation Tissue Area [mm²]
0
2
4
6
*
***
Day 10
No Treatment
Uncoated Scaffold
Coated Scaffold
Cx43 sODN
Cx43 asODN

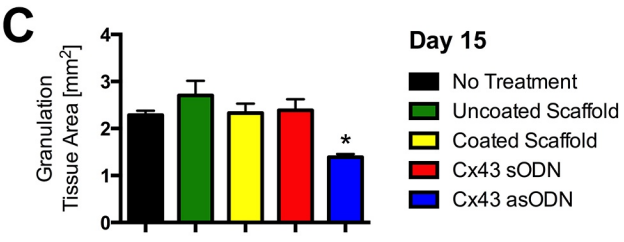
C
Granulation Tissue Area [mm²]
0
1
2
3
4
*
Day 15
No Treatment
Uncoated Scaffold
Coated Scaffold
Cx43 sODN
Cx43 asODN